



**Electrochemical Properties of PVA-GO/PEDOT Nanofibers
Prepared by Electrospinning and Electropolymerization
Techniques**

Journal:	<i>RSC Advances</i>
Manuscript ID	RA-ART-10-2015-021230.R2
Article Type:	Paper
Date Submitted by the Author:	29-Dec-2015
Complete List of Authors:	Sulaiman, Yusran; Univeristi Putra Malaysia, Department of Chemistry Zubair, Nur Afifah; Universiti Putra Malaysia, Department of Chemistry, Faculty of Science Abdul Rahman, Norizah; Universiti Putra Malaysia, Department of Chemistry, Faculty of Science LIM, HONG NGEE; Universiti Putra Malaysia, Department of Chemistry, Faculty of Science Mohd Zawawi, Ruzniza; Universiti Putra Malaysia, Department of Chemistry, Faculty of Science
Subject area & keyword:	Nanomaterials - Materials < Materials



Journal Name

ARTICLE

Electrochemical Properties of PVA-GO/PEDOT Nanofibers Prepared by Electrospinning and Electropolymerization Techniques

Received 00th January 20xx,
Accepted 00th January 20xx

DOI: 10.1039/x0xx00000x

www.rsc.org/

Nur Afifah Zubair,^a Norziah Abdul Rahman,^a Hong Ngee Lim,^{a,b} Ruzniza Mohd Zawawi,^a and Yusran Sulaiman^{a,b*}

Conducting nanofibers composed of poly(vinyl alcohol) (PVA), graphene oxide (GO) and poly(3,4-ethylenedioxythiophene) (PEDOT) were fabricated by a combining method using electrospinning and electropolymerization technique. A small amount of GO was dispersed into PVA as precursor solution for electrospinning, resulting of free-bead nanofiber structures with diameter range less than 200 nm. The SEM images of the obtained nanofiber revealed that PEDOT grew well on the surface of electrospun nanofiber during potentiostatic mode of electropolymerization process. The presence of GO and PEDOT was confirmed by FTIR and Raman spectroscopy analyses. Comparing with the PVA/PEDOT nanofiber, the experimental results indicate that the addition of GO has improved the electrochemical performance of the nanofibers. The electrochemical measurements demonstrated that the PVA-GO/PEDOT composite nanofiber could enhance the current response and reduce the charge transfer resistance of the nanofiber.

1 Introduction

Poly(3,4-ethylenedioxythiophene) (PEDOT) is one of the conducting polymers with tremendous advantages such as high electrical conductivity and environmental stability,¹ low band gap,² enhanced light transmission, and simplicity of production.³ It can be prepared using electrochemical techniques such as cyclic voltammetry, chronoamperometry and chronopotentiometry.^{4, 5} These electroanalytical techniques have several advantages which are required only a small amount of monomer, easy to synthesis, high accuracy of film and short time of polymerization.⁶

Nanofibers are constitute as an interesting material used for a wide range applications such as insulation,⁷ filtration,⁸ drug delivery,⁹ electronic devices and energy storage.¹⁰ Nanofibers have a large surface area to volume ratio and have many interesting properties, such as high surface reactivity, high surface energy, and high thermal and electric conductivity.^{11, 12} Electrospinning process is the most efficient technique for fabrication of polymer nanofiber with small diameter ranging from nanometer to several micrometers.^{13, 14} This technique is

unique as it is able to fabricate nanofibers with controllable of diameter and pore structure, high surface to volume ratio, and the ability to control the nanofiber composition to achieve the desired results from its functionality and properties. Large surface area to volume ratio and its interconnectivity demonstrate that electrospun nanofiber are an excellent material for improving the conductivity of materials.¹¹ In comparison to other common fiber producing techniques like self-assembly,¹⁵ phase separation,¹⁶ wet spinning¹⁷ and extrusion,¹⁸ electrospinning is able to produce ultrathin fibers with very high surface area.¹⁹ Because of these advantages, electrospinning has gained great attention in many applications such as optical, biological scaffolds, wound dressing, and chemical sensors.²⁰

Recently, the production of conducting polymer nanofibers by electrospinning have been widely explored include the introduction of electrospinnable polymer and polymerization of conducting polymers on the surface of electrospun nanofiber to obtain composite nanofibers.^{21, 22} Various polymers such as poly(vinyl alcohol) (PVA),²³ polyacrylonitrile (PAN),²⁴ poly(vinyl pyrrolidone) (PVP)²⁵ have been used. Among them, PVA with a high density of functional hydroxyl groups, also has some excellent properties such as biocompatibility, nontoxicity, processibility and hydrophilicity. The polymerization of conducting polymer on nanofiber has attracted attention due to its electroactive properties that could enhanced the high surface area per volume ratio of the electrospun nanofiber.²¹ Wang et al.²⁶ reported that some nanofillers including single walled and multiwalled carbon nanotubes, montmorillonite and graphene oxide have been added to the polymer matrix to prepare electrospun

^a Department of Chemistry, Faculty of Science, Universiti Putra Malaysia, 43400 UPM Serdang, Selangor, Malaysia.

^b Functional Device Laboratory, Institute of Advanced Technology, Universiti Putra Malaysia, 43400 UPM Serdang, Selangor, Malaysia.

* E-mail: yusran@upm.edu.my. Tel: +60-389466779. Fax: +60-389435380

† Footnotes relating to the title and/or authors should appear here.

Electronic Supplementary Information (ESI) available: [details of any supplementary information available should be included here]. See DOI: 10.1039/x0xx00000x

nanofibers with improved mechanical strength, electrical conductivity, and thermal stability.

An important approach during electrospinning here is to dissolve the nanofiller with the polymer matrix in an appropriate solvent. Since graphene oxide (GO) has abundance of hydrophilic groups on its surface, thus making it as the best candidate for nanofillers to be reinforced with hydrophilic polymer (PVA).

Herein, we report a new facile method to fabricate conductive PVA-GO/PEDOT nanofiber by a combination of two controllable technique, electrospinning and electrochemical polymerization. Electrospun PVA nanofibers incorporated with graphene oxide were prepared and were then coated with the conducting polymer, PEDOT. This study provides a new approach for the cost-effective synthesis of conductive nanomaterial by polymer coating. The morphologies of the fabricated nanofibers were well characterized and the electrochemical performances were investigated by cyclic voltammetry and electrochemical impedance spectroscopy.

2 Experimental Section

Materials

PVA ($M_w = 89,000 \sim 98,000$, 99% hydrolyzed) and 3,4-ethylenedioxythiophene (EDOT, 99%) were purchased from Sigma Aldrich. Lithium perchlorate (LiClO_4) was obtained from Sigma Aldrich. Acetonitrile (CH_3CN , 99%) were purchased from J.T.Baker. Potassium ferricyanide ($\text{K}_3[\text{Fe}(\text{CN})_6]$), potassium ferrocyanide ($\text{K}_4[\text{Fe}(\text{CN})_6]$) and KCl were obtained from BDH Analar. All reagents in this experiment were in analytical grade and used as received without further purification. The indium tin oxide (ITO) glass substrate that consequently used as the electrodes was purchased from Xinyan Technology Ltd. The ITO glass substrates were cleaned by sonication in acetone, ethanol, and deionized water sequentially for 15 min each.

Preparation of graphene oxide

GO was synthesized using a simplified Hummer's method.²⁷ Graphite oxide was obtained by oxidation of graphite flakes in concentrated H_2SO_4 with continuous stirring in ice bath. Then, KMnO_4 was gradually added into the above solution with vigorous stirring for 6 hours. The solution was diluted by addition of deionized water at 80°C . The mixture was stirred for 3 days for complete oxidation of the graphite. The colour of the suspension changed from dark purplish green to dark brown during the oxidation. Distilled water was added into the suspension followed by a few drops of H_2O_2 to stop the oxidation process. The colour of the mixture turned to bright yellow, indicating the high oxidation level of the graphite. The graphite oxide formed was centrifuged at 10,000 rpm and washed with 1.0 M HCl in aqueous solution. Then the centrifuged solution was rinsed three times with deionized water until the pH of the solution become neutral.

Preparation of PVA and PVA-GO nanofibers by electrospinning

PVA solutions with different weight percentage were prepared by dissolving PVA powder in deionized water by stirring for 2 hours at 90°C . GO was added to obtain the concentration of 0.1 mg/mL and the mixture was stirred further for 1 hour in order to disperse the GO suspension completely. The mixture was then sonicated at room temperature for 15 minutes to promote dispersion before electrospinning. PVA solution without the presence of GO was also prepared as comparison. The polymer solution was loaded into glass syringe equipped with a stainless-steel needle attached and injected using a syringe pump at a flow rate of 1.2 mL/h. The collector was a stainless steel metal collector. An ITO glass was attached to the metal collector, whose surface was in the same plane of the collector. The distance between the tip of needle and the collector was about 15 cm. The needle was connected to a high-voltage power supply which operated at 15 kV during electrospinning. The electrospinning was performed in a closed chamber at room temperature. The optimized concentration with smallest diameter and smooth structures of nanofiber was chosen for polymerization of PEDOT.

Electrochemical polymerization of EDOT onto electrospun nanofiber

Electropolymerization of PEDOT onto collected nanofibers was performed in non aqueous medium containing 0.01 M EDOT and 0.1 M LiClO_4 as supporting electrolyte in acetonitrile. A three electrode electrochemical cell was used for electropolymerization. The ITO glass coated with PVA and PVA-GO nanofibers were used as working electrode, platinum wire as counter electrode and silver wire coated with silver chloride as pseudo-reference electrode. The electropolymerization was carried out by using chronoamperometric method with applied potential of 1.2 V for 5 minutes.

Material characterization

The morphology of the nanofibers was observed using scanning electron microscope (JOELSEM, 6400). Samples were gold-coated prior analysis. The dispersion of GO in PVA nanofibers was confirmed by transmission electron microscopy (TEM, S-7100 HITACHI). Raman spectra was obtained with a green laser at 532 nm and Fourier transform infrared spectroscopy (FTIR) was recorded in the range of $4000 - 250 \text{ cm}^{-1}$ at room temperature using attenuated total reflection (ATR) method. Electrochemical properties of PVA-GO/PEDOT nanofiber were studied by using cyclic voltammetry (CV) and electrochemical impedance spectroscopy (EIS) with a three electrode system using ITO glass as working electrode, platinum wire as counter electrode and Ag/AgCl as reference electrode. The electrochemical measurements were carried out at room temperature in $[\text{Fe}(\text{CN})_6]^{3-}$ redox system containing 0.1 M KCl as supporting electrolyte. The CV potential range was scanned from -0.2 V to 0.6 V with scan rate of 0.050 V s^{-1} . Electrochemical impedance spectroscopy (EIS) measurements were carried out in $[\text{Fe}(\text{CN})_6]^{3-/4-}$ redox system containing 0.1 M KCl using a frequency range between 0.01 to 10 kHz at open circuit potential (OCP). The amplitude was set at 5 mV. Both characterizations were carried out by using Metrohm AUTOLAB PGSTAT204.

3 Results and Discussion

Morphologies of nanofibers

The morphology of electrospun nanofibers is controlled by various parameters such as applied voltage, distance between needle tip to collector and the concentration of solution prior electrospinning¹². In this work, the concentration of PVA solution was adjusted from 5 wt% to 20 wt% in the aqueous dispersion which was the feasible range to form nanofiber. The morphological changes of the electrospun fibers are shown in Figure 1. The electrospun fibers showed good fiber morphology without beads on the fiber at the concentration of 10 wt%. At low concentration of PVA (5 wt%), a mixture of fibers and beads was obtained. At this time, electrospay occurs instead of electrospinning due to the high surface tensions and low viscosity of the solution. As shown in Figure 1b-d, the optimum nanofiber size with the smallest diameter can be seen at 10 wt% of PVA with average diameter of 72.11 ± 31.05 nm (Figure 2). Further increase in the concentration of PVA resulted in the formation of continuous uniform nanofibers with larger diameter range between 90 nm to 110 nm. This indicates that the viscosity of the solution and the spinnability increase with the increase in concentration of the solution, which is consistent with the reported literatures.^{12, 28} Hence, 10 wt% of PVA was used for the next study.

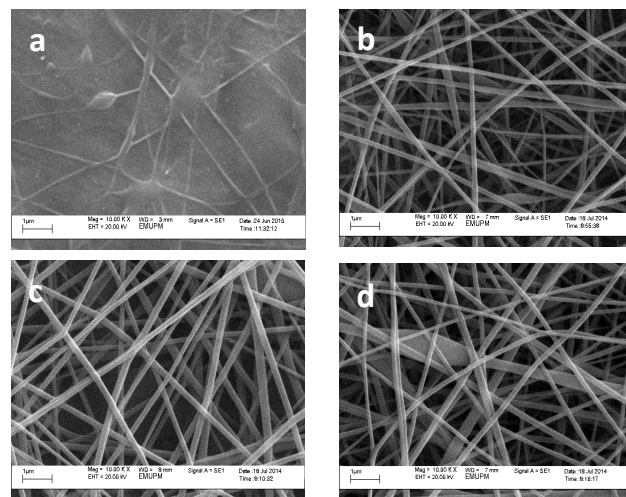


Fig. 1 SEM images of PVA nanofiber fabricated by electrospinning (a) 5wt% PVA (b) 10wt% PVA (c) 15wt% PVA (d) 20wt% PVA

Upon addition of GO (0.1 mg/mL) into 10 wt% of PVA forming PVA-GO nanofiber, it can be seen clearly that that the electrospun nanofibers are smooth with an average diameter of 34.25 ± 12.61 nm (Figure 3a). Most importantly, no beaded structures were observed indicating that PVA containing GO as nanofillers was electrospinnable. The TEM image of electrospun PVA-GO nanofiber (inset Figure 3a) shows a smooth fibrous morphology indicating GO is uniformly distributed in PVA nanofibers. This result is in good agreement with the reported literature.²⁹

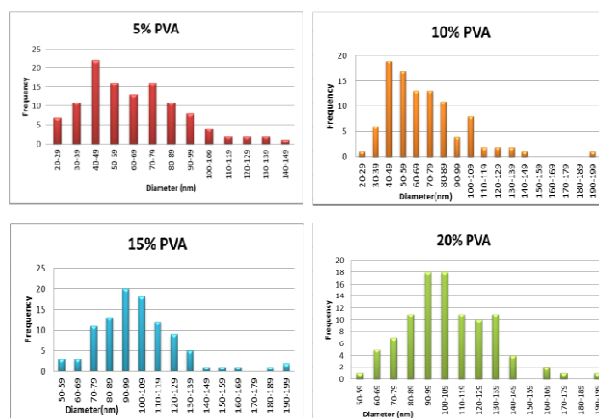


Fig 2 Histogram of the nanofiber diameter distribution for the samples shown in Figure 1.

The electropolymerization of EDOT monomer on the surface of PVA and PVA-GO nanofibers was conducted in non-aqueous medium (acetonitrile) as the PVA nanofibers dissolved in aqueous solution. PEDOT nanostructures were deposited on PVA and PVA-GO by applying a potential of 1.2 V.

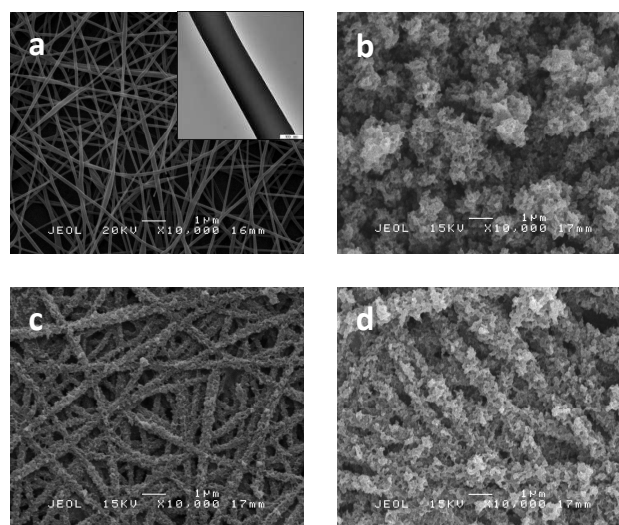


Fig. 3 SEM images (a) PVA-GO (b) PEDOT (c) PVA/PEDOT (d) PVA-GO/PEDOT. Inset: TEM images of PVA-GO nanofiber with magnification of 100,000x.

The SEM images as depicted in Figure 3c-d indicates that aggregated and cauliflower-like structure of PEDOT nanostructures were deposited on PVA and PVA-GO nanofibers with small particle size. It was noticed that the nanofibers displays an increase in diameter after deposition of PEDOT indicating that PEDOT was well coated on the surface of electrospun PVA and PVA-GO nanofiber without disrupted the fibril-like structure of nanofibers. As a comparison, the morphology of PEDOT growth on bare ITO as shown in Figure 3b, which exhibits agglomerated and densely packed structure

with uniform size, which is in agreement with previous reported literature.³⁰

Structural analysis

The FTIR spectra of PVA, GO, PEDOT, PVA/PEDOT, PVA-GO and PVA-GO/PEDOT nanofibers are presented in Figure 4. For pure PVA spectrum (Figure 4a), a broad peak at 3340 cm^{-1} can be attributed to the hydroxyl stretching vibration.²⁶ The characteristic bands of 1112 and 1454 cm^{-1} are attributed to the C-O stretching and C-H bending of PVA, respectively.³¹ The vibrational band observed between 2750 cm^{-1} and 3000 cm^{-1} refers to the stretching of C-H from alkyl groups.³²

A broad peak observed at 3270 cm^{-1} in the spectrum of GO (Figure 4b) corresponds to the strong vibrations of O-H group, whereas the peak observed at 1445 cm^{-1} is due to the symmetric stretching vibrations of C-O from carboxyl group. The small peak appeared at 1190 cm^{-1} represent the C-OH stretching vibration,³³ whereas the peak at 1030 cm^{-1} is the characteristic peak of epoxide group.³⁴ The vibration at 1664 and 1752 cm^{-1} are assigned to the C=C stretching mode and C=O stretching vibration of the carboxyl group, respectively.³⁵

The bands at 632 cm^{-1} and 1110 cm^{-1} in Figure 4c are attributed to the C-S interaction in the thiophene ring, and ethylenedioxy group in PEDOT, respectively.³⁶ As expected, the characteristic peaks of PEDOT at 1840 and 1637 cm^{-1} which attributed to the C-C or C=C stretching of the quinoidal structure of thiophene ring appear in the PVA/PEDOT and PVA-GO/PEDOT spectrum, indicating the presence of PEDOT in the composite nanofibers (Figure 4d-e). These results suggest that PEDOT is coated on PVA and PVA-GO nanofibers during electropolymerization process as supported by the SEM images.

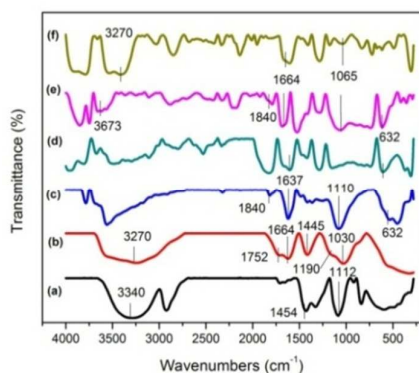


Fig. 4 FTIR spectra of (a) PVA (b) GO (c) PEDOT (d) PVA/PEDOT (e) PVA-GO/PEDOT and (f) PVA-GO

The spectrum of PVA-GO/PEDOT (Figure 4e) shows all the characteristic peaks of individual components. The peak at 632 cm^{-1} is attributed to the C-S bond stretching in thiophene ring which appeared in the spectrum of the PEDOT coated nanofiber. The presence of GO in the nanofibers was confirmed by a peak at 1065 cm^{-1} which assigned to the C-O-C epoxide group in the polymer chains.³⁷ The band observed at 1664 cm^{-1} represent the characteristics peaks for C=C

stretching that presence in GO structure. It should also be noted that the peak due to the O-H within the PVA-GO/PEDOT has shifted to 3673 cm^{-1} which is probably due to the interfacial interaction³⁸ between the GO layers and the PVA chains as illustrated in Figure 6. There is hydrogen bonding between the hydroxyl groups in the PVA chains and the oxygen containing functional groups on the GO surface. The reduction in intensity might be due to the partial removal of OH groups in PVA structures after the dispersion of GO in PVA nanofibers during electrospinning.³⁹

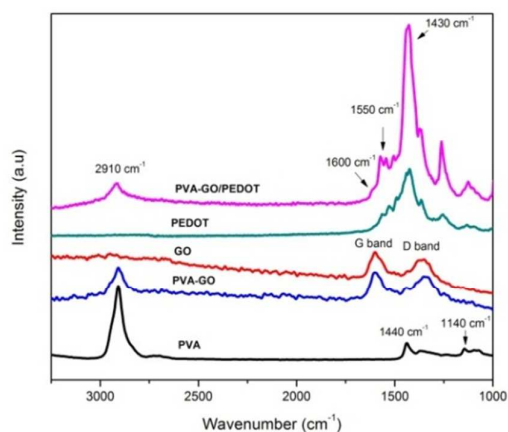


Fig. 5 Raman spectra of (a) PVA (b) PVA-GO (c) GO (d) PEDOT (e) PVA-GO/PEDOT.

Further evidence in the coexistence of the GO and PEDOT in the electrospun nanofiber, Raman spectroscopy measurements were performed as a complementary for FTIR results. For pure PVA, the most intense band centered at 2910 cm^{-1} is originated to the stretching vibrations of CH_2 , and other peaks at 1440 cm^{-1} and 1175 cm^{-1} are assigned to the stretching vibrations of CH and OH in the PVA molecules, respectively.⁴⁰ A vibrational mode at 1140 cm^{-1} can be assigned as the combination of C-O and C-C stretching modes of PVA. The Raman spectrum of PVA-GO nanofibers displays a broad D-band at 1340 cm^{-1} and a broad G-band at 1600 cm^{-1} , which confirms that GO was successfully incorporated into the PVA nanofibers and survived under the electrostatic force and high voltage during electrospinning. The growth of PEDOT on the electrospun nanofiber was confirmed by the presence of two strong bands at 1430 cm^{-1} and 1550 cm^{-1} which are assigned to the asymmetric and symmetric C=C stretching modes, respectively. The Raman bands originating from PEDOT almost overlapped with the G and D bands of GO. However, a hump at 1600 cm^{-1} contributed by G-band can still be observed in the spectrum of PVA-GO/PEDOT. The presence of these peaks revealed that PEDOT was successfully deposited onto PVA-GO nanofibers.

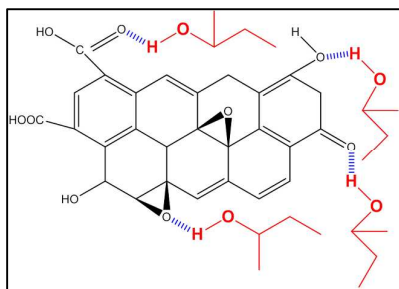


Fig. 6 Possible interaction of PVA-GO nanofiber. GO disperse and forms strong intermolecular hydrogen bonds in the PVA matrix. The functional group of carboxyl, carbonyl, hydroxyl and epoxy in GO structures bind with the hydrogen in PVA chains.

Electrochemical measurements

Cyclic voltammetry was used as a method to study the electrochemical behavior of an electrode. Figure 7 shows the cyclic voltammogram of bare ITO, PEDOT, PVA/PEDOT and PVA-GO/PEDOT modified electrodes in 10 mM $[\text{Fe}(\text{CN})_6]^{3-}$ containing 0.1 M KCl at a scan rate of 50 mV s^{-1} in the range of -0.2 V to 0.6 V . Peak currents were measured relative to extrapolated baseline currents. The bare ITO showed a pair of redox peaks. The peak currents increased obviously after deposition of PEDOT onto the bare ITO surface and electrospun PVA nanofiber, which can be attributed to the good electrical conductivity of PEDOT. The presence of PEDOT enhance the peak current response indicating that the conducting polymer film could accelerate the electron transfer process between the electrochemical probe $[\text{Fe}(\text{CN})_6]^{3-}$ and the ITO. The current was further increased when PEDOT incorporated with PVA-GO, suggesting that GO can provide more electrochemical activity sites.⁴¹ This result may be attributed to the fact that the interaction between GO and the polymer matrices in the nanofiber exhibits excellent reinforcement effects to the nanocomposite materials. The dispersion of GO in the polymer matrices was expected to improve the electrical conductivity and active surface area⁴² of PVA-GO/PEDOT nanofiber, thus resulting of increment in current response. The aggregated and cauliflower-like structure of PEDOT also make the active surface area increased. The diffusion of $[\text{Fe}(\text{CN})_6]^{3-}$ occurs much faster as large surface area of nanofiber provides more reaction sites, results in higher electrochemical reactivity. As can be seen clearly in the Figure 7, the PVA-GO/PEDOT modified electrode gives the highest anodic peak current (i_{pa}) of 550.59 mA at 0.294 V (Table 1).

The effect of peak current on PVA-GO/PEDOT nanofiber was also investigated at different scan rates as shown in Figure 8a. As expected, the redox peak currents increased at higher scan rates, and the anodic (i_{pa}) and cathodic (i_{pc}) peak currents are linearly dependent on the scan rate in the range of 2 to 50 mVs^{-1} with linear regression, R^2 of 0.982 and 0.971 respectively. These results reflect the electrochemical behavior is controlled by the electron transfer,⁴³ since the contribution of diffusion plays an important role on the electrode reaction,

owing to the fact that the electron transfer process of ferricyanide is faster on the PVA-GO/PEDOT modified electrode.

Further analysis of the i_{pa} can be used to determine the types of the redox process. The slopes of 0.50 and 1.00 in a plot of $\log(i_{pa})$ versus \log of peak current (v) are expected for ideal diffusion and surface process, respectively.⁴⁴

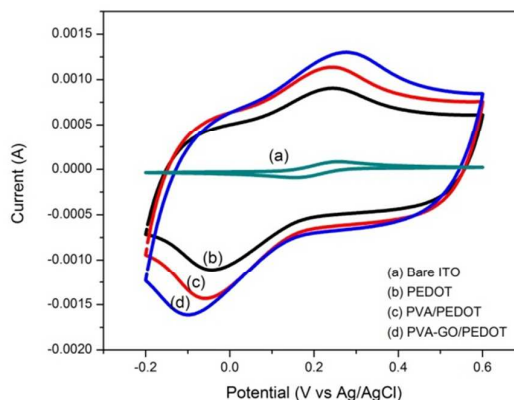


Fig. 7 Cyclic voltammogram of (a) bare ITO (b) PEDOT (c) PVA/PEDOT (d) PVA-GO/PEDOT in 0.01 M $\text{K}_3\text{Fe}(\text{CN})_6$ containing 0.1 M KCl.

In this case, the slope of the $\log(i_{pa})$ versus \log peak current (v) plot (Figure 8c) displayed a linear relationship, with a slope value of 0.4201, suggesting the system tend towards the diffusion-process which is comparable with theoretical slope of 0.5 for diffusion controlled process.^{45, 46} The diffusion controlled process refers to the process of spontaneous transfer of electroactive species (ferricyanide) from the bulk solution (higher concentration) to the electrode surface (lower concentration). Hence, the i_{pa} of PVA-GO/PEDOT nanofiber was assumed to follow the Randles-Sevick equation :

$$i_{pa} = k n^{3/2} A D^{1/2} C^b v^{1/2} \quad (1)$$

where the constant k is equal to 2.69×10^5 , n is the number of moles of electrons transferred per mole of electroactive species $[\text{Fe}(\text{CN})_6]^{3-}$, A is the electrode area in cm^2 , D is the diffusion coefficient in $\text{cm}^2 \text{ s}^{-1}$, C^b is the bulk solution, concentration in mol L^{-1} , and v is the potential scan rate in V s^{-1} . D was determine to be $8.36 \times 10^{-5} \text{ cm}^2/\text{s}$.

Table 1 Value of anodic peak currents, and charge transfer resistance

	i_{pa} (mA)	R_{ct1} (Ω)	R_{ct2} (Ω)	χ^2
PEDOT	357.24	-	8.85	0.050
PVA/PEDOT	445.68	2.47	7.83	0.002
PVA-GO/PEDOT	550.59	1.44	6.32	0.002

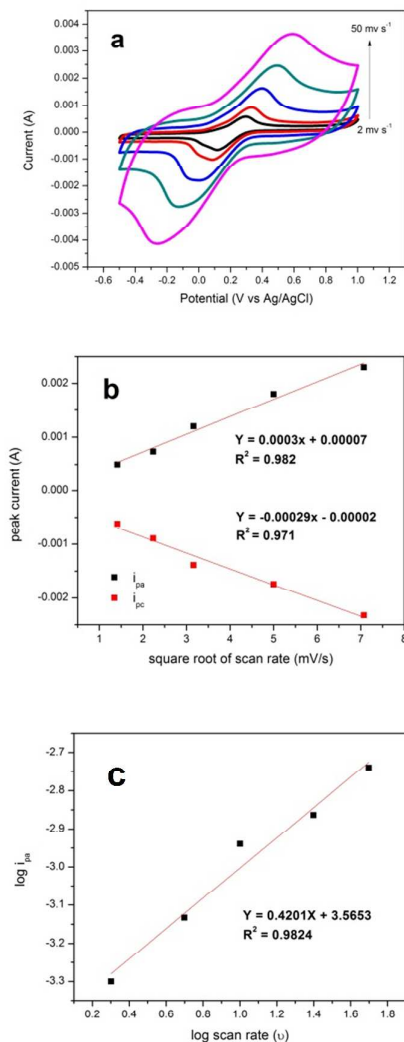


Fig. 8 (a) Cyclic voltammograms of PVA GO/PEDOT in 10 mM $[\text{Fe}(\text{CN})_6]^{3-}$ containing 0.1 M KCl at various scan rates (2, 5, 10, 25, 50 mV s^{-1}) (b) Plot of anodic and cathodic peak current (i_{pa}/i_{pc}) vs square root of scan rate (v) (c) Plot of log of peak current (i_{pa}) vs log of scan rate (v).

In order to investigate the electron transport properties of the modified electrodes, EIS measurements were employed. The Nyquist plots of PEDOT, PVA/PEDOT and PVA-GO/PEDOT are shown in Figure 9. The EIS data were fitted with equivalent electrical circuits (Figure 10) in order to explain the behavior of the electrode and the interface between the nanofiber, PEDOT coated layer and the electrolyte.

The fitting results show small value of chi squared ($\chi^2 \approx 10^{-2}$ to 10^{-3}) indicating that the model is well fitted with the experimental data.⁴⁷ The circuits composed of solution resistance (R_s) which accounts for the resistance of the bulk solution. Constant phase element (CPE) is used to represent the non-ideal behavior of double layer capacitance and inhomogeneity of the electrode surface.⁴⁸ The charge transfer resistance (R_{ct}) is associated with the electron exchange at

electrode-electrolyte interface⁴⁹ while the T element in the equivalent circuits refers to the ion diffusion which correspond to a tangent-hyperbolic function. The proposed model was constructed using component in series. The first component is the R_s , followed by the series combination of CPE and R_{ct} . The equivalent circuits have diffusion element (T) and CPE as the last component which corresponds to the capacitance element.

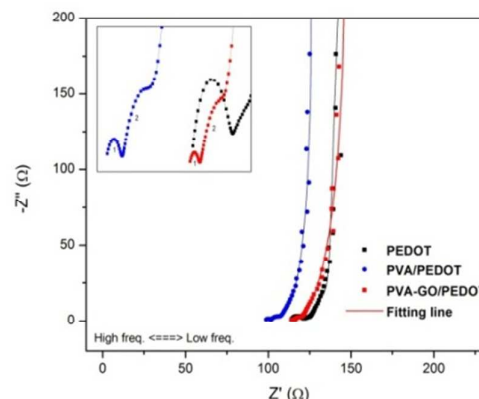


Fig. 9 Nyquist plot of (a) PEDOT (b) PVA/PEDOT (c) PVA-GO/PEDOT in 1.0 mM $[\text{Fe}(\text{CN})_6]^{3-/4-}$ solution containing 0.1 M KCl. The frequency range is from 0.01 to 10^3 Hz.

Based on the spectrum, PEDOT exhibits single semicircle at high frequency region, while two semicircles were observed for PVA/PEDOT and PVA-GO/PEDOT as depicted in Figure 9 (inset). These two semicircles represent the bilayers of the two modified electrodes. The left semicircle (R_{ct1}) was due to the interfacial resistance between the PVA or PVA-GO nanofiber with the PEDOT which found at higher frequencies region, followed by the second semicircle (R_{ct2}) which arises from the charge transfer resistance at the PEDOT|electrolyte interface. For PEDOT, the single semicircle represents the charge transfer resistance at the PEDOT|electrolyte interface.

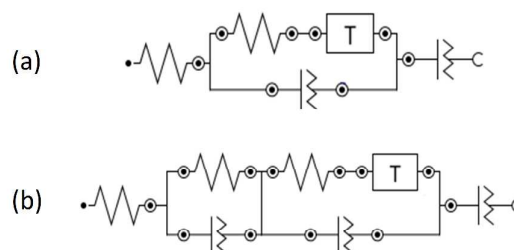


Figure 10. Equivalent electrical circuits for (a) PEDOT and (b) PVA/PEDOT and PVA-GO/PEDOT

The deposition of PEDOT on bare ITO exhibits higher charge transfer resistance (R_{ct}) at the electrode interface among the three modified electrodes. This could be attributed to the agglomeration and compact structures of PEDOT on bare ITO compared to the nanofibrous structures of PVA/PEDOT which provide high surface area and large number of active sites on the electrode surface. The nanostructure of electrospun fiber makes conducting pathways more continuous and uninterrupted, which produce faster electron transportation and higher conductivity. It can be observed by the decreasing of R_{ct} value upon deposition of PEDOT on PVA nanofiber. This value is further decrease for PVA-GO/PEDOT, indicating that the presence of GO could facilitate the electron transfer and exhibit better electrochemical activity.

4 Conclusions

PVA-GO/PEDOT conducting nanofiber was successfully prepared by a combination of electrospinning and electropolymerization methods. Incorporation of GO into the nanofiber was confirmed via FTIR and Raman spectroscopy. The SEM images revealed that the conducting polymer PEDOT was well coated on the electrospun PVA-GO nanofiber. The introduction of GO into the electrospinning solution exhibits good electrochemical performances which caused by the high active surface area and conducting pathway on the surface of nanofiber. PVA-GO/PEDOT showed better electrochemical performance that can be used as a new sensing platform.

Acknowledgements

This research work was supported by Universiti Putra Malaysia Grant (GP-IPB/2013/9412701).

References

1. K. Fehse, K. Walzer, K. Leo, W. Lövenich and A. Elschner, *Advanced Materials*, 2007, **19**, 441-444.
2. X. Zhang, J.-S. Lee, G. S. Lee, D.-K. Cha, M. J. Kim, D. J. Yang and S. K. Manohar, *Macromolecules*, 2006, **39**, 470-472.
3. L. Groenendaal, F. Jonas, D. Freitag, H. Pielartzik and J. R. Reynolds, *Advanced Materials*, 2000, **12**, 481-494.
4. N. Sakmeche, S. Aeiayach, J.-J. Aaron, M. Jouini, J. C. Lacroix and P.-C. Lacaze, *Langmuir*, 1999, **15**, 2566-2574.
5. Y. Sulaiman and R. Katakya, *Journal of The Electrochemical Society*, 2012, **159**, F1-F9.
6. C. R. Siju, K. N. Rao and S. Sindhu, *Journal of Optics*, 2013, **42**, 67-72.
7. T. Miki, Y. Murasawa, B. Aronggaowa, Y. Ota, S. Heike, T. Hashizume and T. Shimomura, *Synthetic Metals*, 2013, **175**, 200-204.
8. S. Sundarrajan, K. L. Tan, S. H. Lim and S. Ramakrishna, *Procedia Engineering*, 2013, **75**, 159-163.
9. X. Hu, S. Liu, G. Zhou, Y. Huang, Z. Xie and X. Jing, *Journal of Controlled Release*, 2014, **185**, 12-21.
10. M. Kumar, A. Subramania and K. Balakrishnan, *Electrochimica Acta*, 2014, **149**, 152-158.
11. S. Ramakrishna, K. Fujihara, W.-E. Teo, T. Yong, Z. Ma and R. Ramaseshan, *Materials Today*, 2006, **9**, 40-50.
12. N. Bhardwaj and S. C. Kundu, *Biotechnology Advances*, 2010, **28**, 325-347.
13. Y. C. Ahn, S. K. Park, G. T. Kim, Y. J. Hwang, C. G. Lee, H. S. Shin and J. K. Lee, *Current Applied Physics*, 2006, **6**, 1030-1035.
14. S. Sen, F. J. Davis, G. R. Mitchell and E. Robinson, *Journal of Physics: Conference Series*, 2009, **183**, 012020.
15. R. Vasita and D. S. Katti, *International Journal of Nanomedicine*, 2006, **1**, 15-30.
16. J. Zhao, W. Han, M. Tu, S. Huan, R. Zeng, H. Wu, Z. Cha and C. Zhou, *Materials Science and Engineering: C*, 2012, **32**, 1496-1502.
17. L. Kong and G. R. Ziegler, *Food Hydrocolloids*, 2014, **38**, 220-226.
18. C. H. Xue, D. Wang, B. Xiang, B.-S. Chiou and G. Sun, *Materials Chemistry and Physics*, 2010, **124**, 48-51.
19. A. Greiner and J. H. Wendorff, *Angewandte Chemie International Edition*, 2007, **46**, 5670-5703.
20. Z.-M. Huang, Y. Z. Zhang, M. Kotaki and S. Ramakrishna, *Composites Science and Technology*, 2003, **63**, 2223-2253.
21. K. H. Hong, K. W. Oh and T. J. Kang, *Journal of Applied Polymer Science*, 2005, **96**, 983-991.
22. J. E. Yang, I. Jang, M. Kim, S. H. Baeck, S. Hwang and S. E. Shim, *Electrochimica Acta*, 2013, **111**, 136-143.
23. N. T. B. Linh, Y. K. Min, H.-Y. Song and B.-T. Lee, *Journal of Biomedical Materials Research Part B: Applied Biomaterials*, 2010, **95B**, 184-191.
24. S. Y. Gu, J. Ren and Q. L. Wu, *Synthetic Metals*, 2005, **155**, 157-161.
25. J. Bai, Y. Li, L. Sun, C. Zhang and Q. Yang, *Bulletin of Materials Science*, 2009, **32**, 161-164.
26. B. Wang, Z. Chen, J. Zhang, J. Cao, S. Wang, Q. Tian, M. Gao and Q. Xu, *Colloids and Surfaces A: Physicochemical and Engineering Aspects*, 2014, **457**, 318-325.
27. N. M. Huang, H. N. Lim, C. H. Chia, M. A. Yarmo and M. R. Muhamad, *International Journal of Nanomedicine*, 2011, **6**, 3443-3448.
28. H. Fong, I. Chun and D. H. Reneker, *Polymer*, 1999, **40**, 4585-4592.
29. Y. Y. Qi, Z. X. Tai, D. F. Sun, J. T. Chen, H. B. Ma, X. B. Yan, B. Liu and Q. J. Xue, *Journal of Applied Polymer Science*, **127**, 1885-1894.

- 30 S. Patra, K. Barai and N. Munichandraiah, *Synthetic Metals*, 2008, **158**, 430-435.
- 31 S. Abbasizadeh, A. R. Keshtkar and M. A. Mousavian, *Chemical Engineering Journal*, 2013, **220**, 161-171.
- 32 H. S. Mansur, C. M. Sadahira, A. N. Souza and A. A. P. Mansur, *Materials Science and Engineering: C*, 2008, **28**, 539-548.
- 33 A. Grinou, Y. Yun and H.-J. Jin, *Macromolecular Research*, 2011, **20**, 84-92.
- 34 C. Zhu, J. Zhai, D. Wen and S. Dong, *Journal of Materials Chemistry*, 2012, **22**, 6300-6306.
- 35 Q. Xu, Y. Li, W. Feng and X. Yuan, *Synthetic Metals*, 2009, **160**, 88-93.
- 36 S. Selvaganesh, J. Mathiyarasu, K. L. N. Phani and V. Yegnaraman, *Nanoscale Research Letters*, 2007, **2**, 546 - 549.
- 37 P. Manivel, M. Dhakshnamoorthy, A. Balamurugan, N. Ponpandian, D. Mangalaraj and C. Viswanathan, *RSC Advances*, 2013, **3**, 14428-14437.
- 38 X. Qi, X. Yao, S. Deng, T. Zhou and Q. Fu, *Journal of Materials Chemistry A*, 2013, **2**, 2240-2249.
- 39 E. Marin and J. Rojas, *International Journal of Pharmacy and Pharmaceutical Sciences*, 2014, **7**.
- 40 Y. A. Badr, K. M. Abd El-Kader and R. M. Khafagy, *Journal of Applied Polymer Science*, 2004, **92**, 1984-1992.
- 41 F. Jiang, Z. Yao, R. Yue, Y. Du, J. Xu, P. Yang and C. Wang, *International Journal of Hydrogen Energy*, 2012, **37**, 14085-14093.
- 42 R. Thangappan, S. Kalaiselvam, A. Elayaperumal and R. Jayavel, *Solid State Ionics*, 2014, **268**, Part B, 321-325.
- 43 L. Shahriary and A. A. Athawale, *IJREEE*, 2014, **2**, 58-63.
- 44 N. S. Lawrence, R. P. Deo and J. Wang, *Analytical Chemistry*, 2004, **76**, 3735-3739.
- 45 N. G. Shang, P. Papakonstantinou, M. McMullan, M. Chu, A. Stamboulis, A. Potenza, S. S. Dhesi and H. Marchetto, *Advanced Functional Materials*, 2008, **18**, 3506-3514.
- 46 L. Tang, Y. Wang, Y. Li, H. Feng, J. Lu and J. Li, *Advanced Functional Materials*, 2009, **19**, 2782-2789.
- 47 M. Ates, *Progress in Organic Coatings*, 2011, **71**, 1-10.
- 48 D. Giray, T. Balkan, B. Dietzel and A. Sezai Sarac, *European Polymer Journal*, 2013, **49**, 2645-2653.
- 49 N. Yasri, A. K. Sundramoorthy, W.-J. Chang and S. Gunasekaran, *Frontiers in Materials*, 2014, **1**.